

Astrocyte Autophagy Flux Protects Neurons Against Oxygen-Glucose Deprivation and Ischemic/Reperfusion Injury

Authors:

Xue Liu, Fengfeng Tian, Shiquan Wang, Feng Wang*, Lize Xiong*

Authors affiliations:

Department of Anesthesiology and Perioperative Medicine, Xijing Hospital, Fourth Military Medical University, Xi'an, 710032, China

Corresponding author:

Address correspondence and reprint requests to Dr. Feng Wang and Dr. Lize Xiong, Department of Anesthesiology and Perioperative Medicine, Xijing Hospital, The Fourth Military Medical University Xi'an, China 710032.

Tel: +86 029 84775337 Fax: +86 029 84775337 E-mail: maple515@sina.com

Tel: +86 029 84775343 Fax: +86 029 84775337 E-mail: mzkxlz@126.com

This article has been peer-reviewed and accepted for publication, but has yet to undergo copyediting and proof correction. The final published version may differ from this proof. Downloaded by Kings College London-Journal Section from online.liebertpub.com at 11/11/17. For personal use only.

Rejuvenation Research

Astrocyte Autophagy Flux Protects Neurons Against Oxygen-Glucose Deprivation and Ischemic/Reperfusion Injury (DOI: 10.1089/rej.2017.1999)

This paper has been peer-reviewed and accepted for publication, but has yet to undergo copyediting and proof correction. The final published version may differ from this proof.

Abstract

The role of autophagy varies with the type of acute brain injury. In general, autophagy mediates a clear neuroprotective effect in intoxication caused by various psychoactive agents, subarachnoid hemorrhage and spinal cord injury. In contrast, autophagic cell death has also been reported to actively contribute to neuronal loss in neonatal hypoxic ischemic encephalopathy. However, it still remains to be determined whether autophagy plays a cytoprotective or a cytotoxic role in stroke. Previous studies focused primarily on the role of neurons rather than the role of astrocytes in brain injury. Thus, it is unknown whether modulating the autophagy flux of astrocytes contributes to improving neuronal survival after stroke. In the current study, we investigated the time course of autophagy flux in vitro using co-cultured astrocytes and neurons exposed to oxygen-glucose deprivation/re-oxygenation which mimicked the process of ischemia/reperfusion. Autophagy flux of astrocytes was regulated by treatment with the autophagy inducer rapamycin, autophagy inhibitor 3-methyladenine, and the transduction of small interfering RNA against autophagy-related gene 5. In addition, AAV-GFAP-ATG7 was used to induce astrocyte autophagy flux in mice subjected to focal cerebral ischemia. We found that induction of autophagy flux of astrocytes in vitro enhanced the viability of neurons and decreased neuronal apoptosis. Furthermore, induction of astrocyte autophagy flux in mice improved neurological outcomes. In contrast, inhibition of autophagy flux in astrocytes decreased the viability of neurons and increased neuronal apoptosis. These results suggest that upregulation of autophagy flux in astrocytes may contribute to endogenous neuroprotective and neurorecovery mechanisms after stroke.

Keywords: Astrocytes; Autophagy flux; Neurons; Co-cultures; Oxygen glucose deprivation/re-oxygenation; Ischemia/reperfusion

Introduction

Autophagy is a cytoplasmic bulk degradation pathway that is part of a dynamic recycling system that produces new building blocks and energy for cellular rejuvenation and homeostasis. Autophagy involved in many vital physiological and pathological processes^{1, 2}. The term “autophagy flux” signifies the process of autophagosome synthesis, delivery of autophagy substrates to lysosomes, and degradation of autophagy substrates inside lysosomes³. Canonical autophagy is regulated by various autophagy-related genes (ATG) that are evolutionarily highly conserved⁴ and control, controlling the sequential steps of autophagy⁵. Microtubule-associated protein 1 light chain 3 (MAP1LC3), a mammalian ortholog of yeast ATG8, is a ubiquitin-like protein that exists in 2 different forms. Cytosolic-LC3- I and phospholipid-conjugated, LC3- II⁶. Levels of LC3- II are highly correlated with the number of autophagosomes⁷ and serve as an indicator of autophagosome formation. However, *Atg5* and *Atg7* genes are also involved in autophagy induction and autophagosome formation.

Constitutive autophagy flux in neurons plays essential roles in key neuronal processes under physiological conditions at baseline levels. However, it is activated rapidly in neurons subjected to hypoxic conditions⁸, excitotoxic stimuli⁹, closed head injuries¹⁰ or focal cerebral ischemia¹¹. A recent study has suggested that autophagy flux involved in a neuronal death pathway following ischemic brain injury¹². However, previous studies have yielded conflict results on the role of autophagy in brain injury in that both suppression and induction of autophagy flux by pharmaceuticals reduced the severity of brain injury in rodents¹³⁻¹⁵. The novel contributions of the paper involve improvements in our understanding of the role of astrocyte autophagy flux in oxygen-glucose deprivation or ischemia/reperfusion. It is the first paper that address this question.

Astrocytes play a key role in evolution of the complexity of nervous system function¹⁶. Homeostasis of astrocytes is critical to neurons, especially during cerebral ischemia¹⁸, and autophagy flux plays an important role in maintaining astrocyte homeostasis². It was reported that activation of autophagy after ischemia/reperfusion could be induced in neurons and astrocytes, but not in the microglial cells¹⁹. The dynamic balance of

autophagy flux in astrocytes is necessary to ensure their basic functions. Therefore, we are very interested in investigating how different levels of autophagy flux in astrocytes affect neurons subjected to oxygen-glucose deprivation (OGD) and transient focal cerebral ischemia.

The importance of astrocyte-neuron interactions is supported by considerable evidence^{20, 21}. This study aimed to increase the neuronal survival rate following OGD and ischemic injury by regulating autophagy flux in astrocytes via administration of the autophagy inducer rapamycin (RAPA), autophagy inhibitor 3-methyladenine (3-MA), small interfering RNA (siRNA) against autophagy-related gene 5 (siATG5), AAV-GFAP-ATG7. We found that upregulation of autophagy flux in astrocytes with RAPA or AAV-GFAP-ATG7 resulted in cytoprotection and neuroprotection.

Materials and Methods

Isolation and culture of astrocytes

Primary astrocytes for cell culture were isolated from the cerebral cortex of C57BL6 mice on postnatal day 1-3 (P1-3). Briefly, P1-3 pups were sterilized in 75% alcohol and euthanized by rapid decapitation. The meninges were discarded, and the cerebral cortices and hippocampi were retained. Tissues from 6 mice were minced and transferred to a solution containing 0.25% trypsin (Beyotime, Jiangsu, China, C0201). Cells were extracted using a single 10-min incubations with trypsin supplemented with DNase 1 (Beyotime). Next, cells were pelleted using low-speed centrifugation (1,000 rpm, 5 min) and resuspended in Dulbecco's Modified Eagle's Medium (DMEM, Invitrogen) supplemented with 10% fetal bovine serum and a mixture of 100 U/mL penicillin and 100 µg/mL streptomycin. We plated dissociated cells on 2 T75 flasks evenly coated with poly-L-lysine (Sigma-Aldrich, St Louis, MO, USA, P1399). Prior to astrocyte planting, flasks were coated for at least 6 h in a 40 µg/mL solution of poly-L-lysine in deionized water in a 37°C incubator and then washed 3 times with sterile deionized water. On the third day after plating, the culture medium was replaced completely and purified by incubator shaker (37°C, 240 bpm, 19 h). Some cells from each astrocyte isolation were plated onto 8 mm

cover slips in 24 well plates coated with poly-L-lysine using previously described methods to determine astrocyte purity and regulate autophagy flux levels through administration of agents or lentivirus. Astrocytes cultured in T75 flasks were utilized only when the corresponding glass cover slips showed astrocyte purity > 95%. The astrocyte cell type was confirmed using an anti-glial fibrillary acidic protein (GFAP) stain. The immunofluorescence staining procedure is described below.

Isolation and culture of primary neurons

Primary neurons for culture were isolated from the cerebral cortex and hippocampus of C57BL6 mice on embryonic day 18–20 (E18–20). The tissues were dissected and dissociated, and neurons were plated at a density of 20,000 cells/cm² on 96-well plates or 24-well coated with poly-L-lysine as described previously²². Neurons were grown in neuronal growth medium, which consisted of Neurobasal medium (Gibco, CA, U.S.) supplemented with 2% B27 (Gibco), 1% glutamine (Gibco) and a mixture of 100 U/mL penicillin and 100 µg/mL streptomycin (Beyotime). On the third day after plating, 50% of the culture medium was replaced. Primary cultures were transduced with lentivirus after 4 days of culture. Oxygen-glucose deprivation/re-oxygenation (OGD/R) experiments were performed on the fourth day of culture or after transduction. Some cultures were treated with RAPA (200 nM) 24 h after transduction. The neuron cell type was confirmed using a microtubule-associated protein 2 (MAP2) stain. The staining procedure is described below.

Neuron-astrocyte co-cultures

First, astrocytes were isolated from the cerebral cortex and hippocampus of newborn mice (< 72 h old) by mechanical dissociation of the tissue. The cultures were maintained in the medium described above and incubated at 37°C in a humidified atmosphere with 5% CO₂. The cultures were initially seeded onto Transwell permeable supports (24- well plate) (Corning, NY, U.S.) and treated with 3-MA, or RAPA for 24 h or transduced with siRNA for 72 h. At this time, neurons were isolated from E18-20 mice, cultured as described above, and plated (5×10^4 /mL) were plated on 96-well or 24- well plates. After three rounds of washing with culture medium, the Transwell support with treated astrocytes were placed over the neurons and the cultures were maintained with neurobasal medium described

above. After establishing the co-cultures, the OGD/R experiments were performed. All animal procedures were performed in accordance with the Fourth Military Medical University Ethical Committee for Animal Experimentation.

Oxygen and glucose deprivation and re-oxygenation (OGD/R)

Primary neurons, astrocytes, or astrocyte-neuron co-cultures were washed 3 times in DMEM without glucose, aspartate, glutamine, or B27 and then incubated in the same DMEM medium. Next, the cells were placed in a modular incubator chamber that was flushed with 2 L/min of a 95% N₂/5% CO₂ gas mixture for 15 min at room temperature to remove oxygen. The chamber was then sealed and placed in a 37°C incubator for 0, 15, 30 or 60 min. Following OGD, the cells were placed in normal medium for 24 h of re-oxygenation under normoxic conditions. For analysis of the results of the culture experiments, we used 4 or 5 cultures and each experiment was performed 4-6 times.

Administration of drugs

Primary astrocytes plated on Transwell permeable supports (24 well plate) were treated with 200 nM RAPA (Sigma-Aldrich, 37094) or 10 mM 3-MA (Sigma-Aldrich, U.S., M9281) for 24 h. Dimethyl sulfoxide (DMSO) at a volume identical to that of the drug treatment was used as the vehicle control. RAPA was dissolved in DMSO as a 100 mM stock solution. 3-MA was dissolved in sterile deionized water as a 100 mM stock solution. Further dilutions were made using culture medium.

RNA interference

siRNAs against ATG5 were purchased from Genechem (Shanghai, China) and transduced into astrocytes to inhibit ATG5 expression. Astrocyte cultures were incubated with ATG5-specific or scramble siRNA according to the manufacturer's instructions. Briefly, astrocytes were infected with lentivirus at a multiplicity of infection of 50. The cells were used for subsequent experiments 72 h after initiation of transfection. Immunoblotting was performed as previously described to confirm a decrease in ATG5 expression.

Staining for immunofluorescence

Cultured primary cells or brain slices were fixed with 4% paraformaldehyde at room temperature. These brains were perfused with paraformaldehyde before mice were euthanized. Primary antibodies were diluted with 5% bovine serum albumin in phosphate-buffered saline (PBS) to prevent non-specific binding. Cells or slices were incubated with primary antibodies at least 24 h at 4°C. The next day, after being washed with PBS, cells or slices were incubated in secondary antibodies for 1.5 h at 37°C. Subsequently, cell nuclei were stained with 4', 6-diamidino-2-phenylindole (DAPI) (Sigma-Aldrich, D8417) for 5 min at room temperature. Primary antibodies and their dilutions were as follows: anti-LC3 1:500 (MBL, PM036), anti-GFAP 1:500 (Cell Signaling Technology, 3670), anti-flag 1:500 (Cell Signaling Technology, 14793), and anti-NeuN 1:500 (GeneTex, GTX30773). Primary antibodies were visualized with a FITC- conjugated secondary antibody against rabbit diluted 1:200 (Jackson ImmunoResearch Laboratories, 120791) or an Alexa Fluor 594 conjugated secondary antibody against mouse diluted 1:500 (Jackson ImmunoResearch Laboratories, U.S., 117783).

Western blots

Expression levels of LC3 and p62 in primary neurons and astrocytes were measured using Western blot analysis. Briefly, soluble lysates of primary neuronal cells were mixed with sample buffer and boiled for 5 min at 95°C. Extracted proteins from cells were separated by 12% SDS-PAGE and then electrophoretically transferred to polyvinylidene difluoride membranes. Subsequently, the membranes were blocked in 5% nonfat milk diluted in Tris-buffered saline containing 0.1% Tween 20 (TBST) for 1 h at room temperature. Western blots were probed with the following antibodies and dilutions: rabbit anti-LC3 1:1000 (MBL, PM036), anti-p62 1:1000 (Sigma-Aldrich, P0067), anti-ATG7 1:1000 (Cell Signaling Technology, D12B11), anti- β -actin 1:1000 (Cwbio, CW0096M) or anti-GAPDH 1:1000 (Cwbio, CW0101) overnight at 4°C. After washing with TBST 3 times, the membranes were incubated with goat anti-mouse IgG 1:10000 (Cwbio, CW0102) or goat anti-rabbit IgG 1:10000 (Cwbio, CW0103) for 1 h. Protein bands were visualized using the ChemiDoc MP Imaging System.

Lactate dehydrogenase (LDH) release assay

After OGD/R, cytotoxicity was analyzed by measuring the activity of LDH released into the medium from damaged cells in the co-culture system. Briefly, the medium containing detached cells was collected and centrifuged. The supernatant was utilized to assess LDH activity, which was measured using an assay kit (Nanjing Jiancheng Bioengineering Institute, China, A020-2) according to the manufacturer's instructions. LDH release was calculated as follows: LDH release (%) = (A positive - A positive blank control)/(A normal - A negative blank) × 100%. Cultures under OGD conditions for 0 min represented basal LDH release and were considered 100%.

Cell viability assay

Neurons, and astrocytes were cultured in 96-well plates and neuron-astrocyte co-cultures were placed in 24-well Transwell plate at 5×10^4 cells per well. OGD was performed as described above. Cell viability was measured by fluorescence chemistry using a 7Sea-Cell Counting Kit (Shanghai 7Sea Pharmatech Co., Ltd, China, C008-3) and a spectrophotometer that determined optical density at 450 nm.

Terminal deoxynucleotidyl transferase-mediated dUTP-digoxigenin nick end labeling (TUNEL) fluorescence

TUNEL assays were performed using an in situ cell death detection kit, TMR red (Roche, Swiss, 2156792) according to the manufacturer's instructions. Briefly, after washing 3 times with PBS, the slides were incubated in permeabilization solution for 2 min on ice. They were then incubated with reaction mixture for 60 min at 37°C. Signals were detected using a fluorescence microscope (Olympus, Japan, BX-51).

Ischemic stroke model

All animal protocols were approved by the Institutional Animal Care and Use Committee of Fourth Military Medical University. A transient ischemia model of 60-min middle cerebral artery occlusion (MCAO) with intraluminal filaments was performed in male C57/BL6 mice (approximately 24 g) using a modified version of a previously described procedure. Briefly, anesthesia was induced with 2% isoflurane in 100% O₂ and maintained with 1% isoflurane.

A 4-0 monofilament nylon suture with a rounded tip was introduced into the external carotid artery lumen and gently advanced into the internal carotid artery until it blocked the bifurcating origin of the MCA. The suture was removed 1 h after MCAO. Test subjects with negligible or moderate ischemic symptoms in any behavior tests on day 1 were excluded, including lack of neurologic deficit and failure to extend the left forepaw fully.

Penumbra injection

Mice that were selected at random were anesthetized with 2% isoflurane by penumbra injection and placed in a stereotaxic frame. A glass electrode was placed stereotaxically into the right penumbra tissue (-1.0 mm posterior to bregma; 1.0 mm lateral, and 0.8 mm below the endocranium). Next, 0.3 μ l of 1.5 \times 10¹² vg/mL AAV-GFAP-GFP or AAV-GFAP-ATG7 (Hanbio Biotechnology Co., Ltd., Shanghai, China) was injected using a 10 μ L Hamilton syringe (Hamilton Co., Reno, NV, USA, 80630). After the injection, the needle was left in place for an additional 5 min before withdrawal. To confirm infection with AAV-GFAP-GFP or AAV-GFAP-ATG7, the brains were harvested and processed for immunostaining.

Evaluation of neurological score and measurement of infarct volume

At 24 h after reperfusion, a 5-point scoring system reported by Longa., et al²³ was used to evaluate neurological deficits in mice: the minimum neurobehavioral score of 0, indicated that the mouse was dead, and the maximum score of 5 indicated that the mouse was normal. The assessment of neurological deficit score was performed by an observer blinded to group information. In an *in vivo* experiment, 54 mice were injected with virus to establish the MCAO model. Finally, 50 mice were considered to satisfy the standard. The mice were then decapitated and the brains were cut into 1-mm-thick coronal sections. The sections were immersed in 2% 2, -3, -5-triphenyltetrazolium chloride (TTC) (Sigma-Aldrich, T8877) at room temperature for 15 min. Unstained areas were defined as infarcts and were measured using image analysis software (Image J). The percentage of infarct volume was calculated using the following formula: (total contralateral hemispheric volume – total ipsilateral hemispheric stained volume)/total contralateral hemispheric volume \times 100.

Statistical analysis

All data, except for neurological scores are presented as means \pm SEM. The statistical significance of differences between the 2 groups was determined by an unpaired Student's *t* test. For all other results containing 3 or more groups, an ANOVA with Tukey's post-hoc analysis was used to determine significance, using Graphpad Prism 6.0 statistics software. Neurological scores were expressed as the median (range) and were analyzed with the Kruskal-Wallis test followed by the Mann-Whitney U-test for multiple comparisons.

Results

The time course of autophagy flux differs in cultured neurons and astrocytes after OGD

We set out to understand the time course of autophagy flux in cultured neurons and in astrocytes after OGD. To do that, primary neurons and astrocytes were cultured separately, and OGD/R model was established. Primary neurons and astrocytes were randomly divided into sham and OGD (1 h)/R (0, 6, 12, 24, or 48 h) groups. In addition, primary astrocytes were randomly divided into sham and OGD (4 h) / R (0, 6, 12, 24, or 48 h) groups. Western blot analysis was used to detect expression of autophagy flux marker proteins LC3 and p62. Under normal conditions, autophagy flux in neurons remained at low levels and was activated immediately upon exposure to OGD and the expression of LC3- II increased (Figure 1A, B). After 12 h, autophagy flux decreased to the baseline level and the expression of LC3- II increased and that of p62 decreased (Figure 1A, C). However, autophagy flux was induced again after oxygenation for 24 h, as well as after 48 h (Figure 1A–C). In contrast, OGD 1 h and re-oxygenation did not cause the autophagy flux level of astrocytes to differ from that of the sham group (Figure 1D–F). Here, we observed a trend for the changes of astrocyte autophagy. Considering the robust feature of astrocytes, we next stimulated astrocyte autophagy with 4 h of OGD. Under normal conditions, autophagy flux in astrocytes remained at high levels (Figure 1G). It was inhibited immediately upon exposure to OGD and decreased to the lowest level after oxygenation for 12 h (Figure 1 G–I). Regarding the decreased expression of LC3- II and the increased expression of p62 (Figure 1G–I). Autophagy flux increased after oxygenation for 24 h as well as after 48 h, returning to baseline levels (Figure 1G–I). Based on these experiments,

we characterized that the time course of changes in autophagy flux in neurons and astrocytes, are very different and that autophagy flux of both cell types reach a stable high level with oxygenation for 24 h after OGD.

Astrocytes enhance viability of neurons after OGD

In order to understand the role of astrocytes in neuronal viability after OGD, we tested the survival of neurons and astrocytes cultured individually, and neurons/astrocytes co-cultured. Viability of neurons cultured alone was assessed at 24 h of re-oxygenation after OGD (60 min). Results showed that neuronal viability was reduced significantly to 65% compared with OGD for 0 min (100%) (Figure 2A). We considered OGD 60 min/re-oxygenation for 24 h an appropriate level of stimulation. In contrast, when astrocytes that had been cultured alone were subjected to OGD (60 min) and after 24 h of re-oxygenation, cell viability showed no significant difference compared with those subjected to OGD for 0 min (Figure 2B). This indicates that astrocytes are more resistant to OGD. Furthermore, the addition of astrocytes to neuronal cell cultures resulted in higher neuronal viability compared with that of neurons cultured alone (Figure 2C), which suggests that astrocytes play a cytoprotective role in OGD/R.

Induction of autophagy flux in astrocytes reduces damage to neurons subjected to OGD

In order to further understand the role of autophagy flux in the transition of astrocytes to neurons during OGD, astrocytes treated with siATG5, 3-MA or RAPA as well as control cells were co-cultured with neurons, and the co-cultures were then subjected to OGD for 0 or 60 min, followed by 24 h of re-oxygenation. LDH release, and cell viability assays as well as TUNEL staining were used to evaluate effects of regulating autophagy flux in astrocytes on co-culture system cytotoxicity and neuronal viability. First, we tested the ability of these treatment with siATG5, 3-MA or RAPA to modulate astrocyte autophagy by detecting the expression of LC3-II via immunofluorescent staining and Western blot analysis. Punctate LC3-positive staining was observed in astrocytes. After administration of RAPA, astrocytes positive for LC3/GFAP (glial fibrillary acidic protein) were activated, and such punctate accumulated in the OGD model (0 min, 60 min)/R (24 h), as indicated by morphological examination and the number of autophagosome compared to Ctrl (Figure

3A, C), whereas treatment with 3-MA or siAtg5 resulted in a significant reduction in autophagosome and LC3- II levels in the OGD/R model (Figure 3A, C). To further confirm that the number of autophagosomes was a indicative of enhanced autophagy flux, immunoblotting showed that LC3- II levels in the primary astrocytes (Figure 3B, D) to be consistent with immunofluorescence. Collectively, 3-MA and siAtg5 resulted in a reduction of autophagy flux level and RAPA resulted in an increase in autophagy flux level in primary astrocytes in OGD/R model.

No significant differences were observed between groups under normal conditions (Figure 4A, B, E and F). However, up-regulation of autophagy flux in astrocytes with RAPA decreased apoptosis (Figure 4C, D) and LDH levels (Figure 4E) and enhanced viability (Figure 4F) of neurons in co-culture. In contrast, downregulation of autophagy flux in astrocytes with 3-MA or siATG5 increased apoptosis (Figure 4C, D) and LDH levels (Figure 4E) and decreased viability (Figure 4F) of neurons in co-culture following OGD for 60 min and re-oxygenation for 24 h. These results suggest that upregulation of autophagy flux in astrocytes reduces co-culture cytotoxicity and promotes neuronal viability, while downregulation of autophagy flux in astrocytes increases co-culture cytotoxicity and decreases neuronal viability after OGD.

Induction of autophagy flux in astrocytes decreases infarct volume and increases neuronal survival after MCAO

To study the effects of modulating autophagy flux of astrocytes on brain infarct volume and neuron survival in animals subjected to MCAO for 1 h and reperfusion for 24 h, wild type C57BL6 mice were divided into AAV-GFAP-GFP and AAV-GFAP-ATG7 groups. An adeno-associated virus (AAV-GFAP-ATG7) that upregulates autophagy flux of astrocytes or a control virus (AAV-GFAP-GFP) was injected into the right penumbra tissue of each mouse. Three weeks later, the ischemia/reperfusion model was established. Before the model was established, we randomly chose 4 mice from each group and assessed the effectiveness of AAV-GFAP-ATG7 by Western blot analysis. AAV-GFAP-ATG7 displayed induction of ATG7 protein, and upregulation of autophagy, as shown by the increased expression of LC3- II (Figure 5A–C). TTC staining was used to measure the brain infarct

volume of each mouse and immunofluorescence was used to assess the survival of neurons in penumbra tissues. Immunostaining confirmed the correct injection site and AAV injection of astrocytes (Figure 6A, B). Upregulation of autophagy flux in astrocytes with AAV-GFAP-ATG7 increased the rate of survival of neurons in penumbra tissue subjected to MCAO/reperfusion injury (Figure 6B, C) and decreased brain infarct volume compared with AAV-GFAP-GFP (Figure 6D, F). However, upregulation of autophagy flux in astrocytes with AAV-GFAP-ATG7 did not affect neurological scores (Figure 6E).

Discussion

In this study, we found that autophagy flux increased in neuron and astrocyte cultures in the OGD model at different time courses, and upregulation of autophagy flux in astrocytes protected neurons subjected to OGD. Similarly, upregulation of autophagy flux in astrocytes by AAV2/9-GFAP-ATG7 played a neuroprotective role in ischemic stroke. One recent study²⁴ reported that neuronal *Atg7* deficiency did not influence stress-related proteins in mice. *Atg5* and *Atg7* are involved in the induction of autophagy and autophagosome formation, without which no autophagy flux can proceed. In *in vitro* experiments, we used siATG5 treatment to modulate the autophagy flux in astrocytes, and we chose AAV-GFAP-ATG7 to modulate autophagy flux in astrocytes in *in vivo* experiments.

Brains of adult mice subjected to ischemia show changes in various biomarkers of autophagy including inhibition of MTORC1, LC3 lipidation, degradation of p62, and upregulation of BECN and LAMP2²⁵⁻²⁷. A previous study showed that the induction of autophagy with RAPA decreased infarct size in mouse models of temporary MCAO (tMCAO) and permanent MCAO (pMCAO). However, similar results were obtained with chloroquine, which is an autophagy inhibitors¹⁴. Moreover, 3-MA increased the loss of neurons in mice subjected to tMCAO, but it exerted a neuroprotective effect in mice with pMCAO²⁸. These observations are inconsistent with the hypothesis that autophagy always exhibits neuroprotective activity in adults cerebral ischemia. Thus, it is important to find another approach to investigate the role of autophagy flux in brain injury. In this study, we examined how compensated astrocyte autophagy flux levels affected neurons via

astrocyte-neuron crosstalk and showed that upregulation of astrocyte autophagy flux levels increased survival of co-cultured neurons after OGD.

Autophagy, which is sometimes referred to type 2 cell death, is a basic cellular process that causes degradation of long-lived proteins and recycling of cellular constituents to ensure survival during starvation or other types of stress. Autophagy upregulated in many tissues during development and is important for survival during neonatal starvation²⁹. Inhibition of autophagy results in accumulation of cytoplasmic abnormal protein inclusion bodies that can cause cell damage and neurodegeneration. Thus, autophagy plays a vital role in cell survival^{30, 31}. ATG5 and ATG7, which are members of the ATG family, play critical roles in autophagy, and are essential proteins in the generation of autophagy flux³²⁻³⁴. Knockdown of ATG5 with siRNA can be used to inhibit activation of autophagy flux.

Previous research has shown that injury due to ischemia/reperfusion can significantly increase autophagy flux levels in astrocytes significantly³⁵. Astrocytes outnumber neurons in the brain¹⁸, and they play essential roles in multiple functions of the central nervous system, including glutamate re-uptake, maintenance of ion and water homeostasis, protection against oxidative stress injury, glycogen energy storage, as well as synapse formation and remodeling^{36, 37}. In addition, astrocytes modulate neuronal activity by releasing gliotransmitters and scavenging glutamate, are involved in synaptic support and formation, and physically contact and connect large numbers of neurons^{20, 38, 39}. Furthermore, our results indicate that astrocytes retain more autophagy machinery function than neurons, as judged by the number of autophagosomes in the cytoplasm, as part of maintaining normal functions. More interestingly, astrocytes are migrating cells⁴⁰, and they bridge structures, such as neurons and vasculature, that otherwise cannot communicate⁴¹. This raises the question of whether autophagy flux in astrocytes is the key to maintaining neuronal survival after OGD or ischemic injury.

Our results suggest that neuronal rescue during recovery from OGD or ischemia is related to the level of autophagy flux in astrocytes. Immunofluorescence staining showed decreased numbers of apoptotic cells and increased neuronal viability and survival, which suggests that upregulation of autophagy flux levels in astrocytes increases neuronal

survival. However, the causal relationships among these observations are unclear, and further investigations are needed to elucidate the underlying mechanism. Autophagy may serve as a homeostatic mechanism to inhibit apoptosis and limit adverse effects of chronic ischemia⁴². Induction of autophagy flux in cells decreases the activation of pro-apoptotic Bax, whereas suppression of autophagy via knockdown of ATG5 or 3-MA increases cellular damage, suggesting that autophagy serves as a protective mechanism against ischemia/reperfusion⁴³. The critical role of astrocytes in the central nervous system is well known⁴⁴, and effects of abnormal astrocytes on neurons have been studied widely. The stability of astrocytes is of great significance to neurons, especially in cerebral ischemia.

Previous studies focused on inducing or suppressing autophagy flux in neurons, and the results were controversial. In contrast, this study examined how regulating autophagy flux in astrocytes affects neurons. We showed that induction of autophagy flux in astrocytes reduced neuronal cell death, while inhibition of autophagy flux in astrocytes increased neuronal cell death. Because both 3-MA and RAPA have limited specificity for regulating autophagy flux, it is important to use more specific methods to inhibit autophagy. Thus, we also used genetic knockdown of ATG5 to downregulate astrocyte autophagy flux and AAV-GFAP-ATG7 to upregulate astrocyte autophagy flux, which are critical ATG genes.

In conclusion, this study explored how regulating astrocyte autophagy flux affects neurons, and results suggest that astrocyte autophagy flux may protect neurons from OGD or ischemic injury. However, the mechanism underlying the observed significant effects of astrocyte autophagy flux levels in astrocytes on neurons remains unknown. In general, the crosstalk between astrocytes and neurons in the context of autophagy flux level regulation remains unclear. Neuron-astrocyte interactions are vital for normal functions and viability of neurons and should be elucidated further regarding neuroprotective mechanisms such as autophagy. Nonetheless, our findings suggest that upregulation of autophagy flux in astrocytes may be a promising strategy that should be developed in depth in the hope of improving prognosis of stroke patients. It is essential to explore the pathway underlying the protective effects of upregulating autophagy flux in astrocytes in OGD-induced neuronal damage.

Declaration of interest

The authors declare that there are no conflicts of interest that could be perceived as prejudicing the impartiality of the reported research.

Acknowledgments

This project was supported by the Funds for International Cooperation and Exchange of the National Natural Science Foundation of China (No. 81420108013), and the Changjiang Scholars and Innovative Research Team in University, Xi'an, China (No. IRT-14R08).

References

1. Mizushima N, and Komatsu M. Autophagy: renovation of cells and tissues. *Cell*. 2011;147(4):728-41.
2. Boya P, Reggiori F, and Codogno P. Emerging regulation and functions of autophagy. *Nat Cell Biol*. 2013;15(7):713-20.
3. Castillo K, Valenzuela V, Matus S, Nassif M, Onate M, Fuentealba Y, Encina G, Irrazabal T, Parsons G, Court FA, et al. Measurement of autophagy flux in the nervous system in vivo. *Cell Death Dis*. 2013;4(e917).
4. Noda NN, Ohsumi Y, and Inagaki F. ATG systems from the protein structural point of view. *Chem Rev*. 2009;109(4):1587-98.
5. Deretic V, Saitoh T, and Akira S. Autophagy in infection, inflammation and immunity. *Nat Rev Immunol*. 2013;13(10):722-37.
6. Mizushima N, and Yoshimori T. How to interpret LC3 immunoblotting. *Autophagy*. 2007;3(6):542-5.
7. Tanida I, Minematsu-Ikeguchi N, Ueno T, and Kominami E. Lysosomal turnover, but not a cellular level, of endogenous LC3 is a marker for autophagy. *Autophagy*. 2005;1(2):84-91.
8. Sakai K, Fukuda T, and Iwadata K. Immunohistochemical analysis of the ubiquitin proteasome system and autophagy lysosome system induced after traumatic intracranial injury: association with time between the injury and death. *Am J Forensic Med Pathol*. 2014;35(1):38-44.
9. Wang Y, Han R, Liang ZQ, Wu JC, Zhang XD, Gu ZL, and Qin ZH. An autophagic mechanism is involved in apoptotic death of rat striatal neurons induced by the non-N-methyl-D-aspartate receptor agonist kainic acid. *Autophagy*. 2008;4(2):214-26.
10. Diskin T, Tal-Or P, Erlich S, Mizrachy L, Alexandrovich A, Shohami E, and Pinkas-Kramarski R. Closed head injury induces upregulation of Beclin 1 at the cortical site of

injury. *J Neurotrauma*. 2005;22(7):750-62.

11. Rami A, Langhagen A, and Steiger S. Focal cerebral ischemia induces upregulation of Beclin 1 and autophagy-like cell death. *Neurobiol Dis*. 2008;29(1):132-41.
12. Carloni S, Buonocore G, and Balduini W. Protective role of autophagy in neonatal hypoxia-ischemia induced brain injury. *Neurobiol Dis*. 2008;32(3):329-39.
13. Baek SH, Noh AR, Kim KA, Akram M, Shin YJ, Kim ES, Yu SW, Majid A, and Bae ON. Modulation of mitochondrial function and autophagy mediates carnosine neuroprotection against ischemic brain damage. *Stroke*. 2014;45(8):2438-43.
14. Buckley KM, Hess DL, Sazonova IY, Periyasamy-Thandavan S, Barrett JR, Kirks R, Grace H, Kondrikova G, Johnson MH, Hess DC, et al. Rapamycin up-regulation of autophagy reduces infarct size and improves outcomes in both permanent MCAO, and embolic MCAO, murine models of stroke. *Exp Transl Stroke Med*. 2014;6(8).
15. Lee JA, and Gao FB. Inhibition of autophagy induction delays neuronal cell loss caused by dysfunctional ESCRT-III in frontotemporal dementia. *J Neurosci*. 2009;29(26):8506-11.
16. Freeman MR, and Rowitch DH. Evolving concepts of gliogenesis: a look way back and ahead to the next 25 years. *Neuron*. 2013;80(3):613-23.
17. Attwell D, Buchan AM, Charkpak S, Lauritzen M, Macvicar BA, and Newman EA. Glial and neuronal control of brain blood flow. *Nature*. 2010;468(7321):232-43.
18. Bambrick L, Kristian T, and Fiskum G. Astrocyte mitochondrial mechanisms of ischemic brain injury and neuroprotection. *Neurochem Res*. 2004;29(3):601-8.
19. Tian F, Deguchi K, Yamashita T, Ohta Y, Morimoto N, Shang J, Zhang X, Liu N, Ikeda Y, Matsuura T, et al. In vivo imaging of autophagy in a mouse stroke model. *Autophagy*. 2014;6(8):1107-14.
20. Filosa A, Paixao S, Honsek SD, Carmona MA, Becker L, Feddersen B, Gaitanos L, Rudhard Y, Schoepfer R, Klopstock T, et al. Neuron-glia communication via EphA4/ephrin-

A3 modulates LTP through glial glutamate transport. *Nat Neurosci.* 2009;12(10):1285-92.

21. Kaczor P, Rakus D, and Mozrzymas JW. Neuron-astrocyte interaction enhance GABAergic synaptic transmission in a manner dependent on key metabolic enzymes. *Front Cell Neurosci.* 2015;9(120).

22. Tsvetkov AS, Miller J, Arrasate M, Wong JS, Pleiss MA, and Finkbeiner S. A small-molecule scaffold induces autophagy in primary neurons and protects against toxicity in a Huntington disease model. *Proc Natl Acad Sci U S A.* 2010;107(39):16982-7.

23. Longa EZ, Weinstein PR, Carlson S, and Cummins R. Reversible middle cerebral artery occlusion without craniectomy in rats. *Stroke.* 1989;20(1):84-91.

24. Xie C, Ginet V, Sun Y, Koike M, Zhou K, Li T, Li H, Li Q, Wang X, Uchiyama Y, et al. Neuroprotection by selective neuronal deletion of Atg7 in neonatal brain injury. *Autophagy.* 2016;12(2):410-23.

25. Liu N, Shang J, Tian F, Nishi H, and Abe K. In vivo optical imaging for evaluating the efficacy of edaravone after transient cerebral ischemia in mice. *Brain Res.* 2011;1397(66-75).

26. Li WL, Yu SP, Chen D, Yu SS, Jiang YJ, Genetta T, and Wei L. The regulatory role of NF-kappaB in autophagy-like cell death after focal cerebral ischemia in mice. *Neuroscience.* 2013;244(16-30).

27. Mehta SL, Lin Y, Chen W, Yu F, Cao L, He Q, Chan PH, and Li PA. Manganese superoxide dismutase deficiency exacerbates ischemic brain damage under hyperglycemic conditions by altering autophagy. *Transl Stroke Res.* 2011;2(1):42-50.

28. Zhang X, Yan H, Yuan Y, Gao J, Shen Z, Cheng Y, Shen Y, Wang RR, Wang X, Hu WW, et al. Cerebral ischemia-reperfusion-induced autophagy protects against neuronal injury by mitochondrial clearance. *Autophagy.* 2013;9(9):1321-33.

29. Kuma A, Hatano M, Matsui M, Yamamoto A, Nakaya H, Yoshimori T, Ohsumi Y, Tokuhisu T, and Mizushima N. The role of autophagy during the early neonatal starvation period. *Nature.* 2004;432(7020):1032-6.

30. Hara T, Nakamura K, Matsui M, Yamamoto A, Nakahara Y, Suzuki-Migishima R, Yokoyama M, Mishima K, Saito I, Okano H, et al. Suppression of basal autophagy in neural cells causes neurodegenerative disease in mice. *Nature*. 2006;441(7095):885-9.
31. Komatsu M, Waguri S, Chiba T, Murata S, Iwata J, Tanida I, Ueno T, Koike M, Uchiyama Y, Kominami E, et al. Loss of autophagy in the central nervous system causes neurodegeneration in mice. *Nature*. 2006;441(7095):880-4.
32. Besirli CG, Chinsky ND, Zheng QD, and Zacks DN. Autophagy activation in the injured photoreceptor inhibits fas-mediated apoptosis. *Invest Ophthalmol Vis Sci*. 2011;52(7):4193-9.
33. Pyo JO, Jang MH, Kwon YK, Lee HJ, Jun JI, Woo HN, Cho DH, Choi B, Lee H, Kim JH, et al. Essential roles of Atg5 and FADD in autophagic cell death: dissection of autophagic cell death into vacuole formation and cell death. *J Biol Chem*. 2005;280(21):20722-9.
34. Hammond EM, Brunet CL, Johnson GD, Parkhill J, Milner AE, Brady G, Gregory CD, and Grand RJ. Homology between a human apoptosis specific protein and the product of APG5, a gene involved in autophagy in yeast. *FEBS Lett*. 1998;425(3):391-5.
35. Klionsky DJ, Abdelmohsen K, Abe A, Abedin MJ, Abeliovich H, Acevedo Arozena A, Adachi H, Adams CM, Adams PD, Adeli K, et al. Guidelines for the use and interpretation of assays for monitoring autophagy (3rd edition). *Autophagy*. 2016;12(1):1-222.
36. Ransom BR, and Ransom CB. Astrocytes: multitalented stars of the central nervous system. *Methods Mol Biol*. 2012;814(3-7).
37. Kim K, Lee SG, Kegelmann TP, Su ZZ, Das SK, Dash R, Dasgupta S, Barral PM, Hedvat M, Diaz P, et al. Role of excitatory amino acid transporter-2 (EAAT2) and glutamate in neurodegeneration: opportunities for developing novel therapeutics. *J Cell Physiol*. 2011;226(10):2484-93.
38. Lalo U, Rasooli-Nejad S, and Pankratov Y. Exocytosis of gliotransmitters from cortical astrocytes: implications for synaptic plasticity and aging. *Biochem Soc Trans*. 2014;42(5):1275-81.

39. Chung WS, Clarke LE, Wang GX, Stafford BK, Sher A, Chakraborty C, Joung J, Foo LC, Thompson A, Chen C, et al. Astrocytes mediate synapse elimination through MEGF10 and MERTK pathways. *Nature*. 2013;504(7480):394-400.
40. Jacobsen CT, and Miller RH. Control of astrocyte migration in the developing cerebral cortex. *Dev Neurosci*. 2003;25(2-4):207-16.
41. Zonta M, Angulo MC, Gobbo S, Rosengarten B, Hossmann KA, Pozzan T, and Carmignoto G. Neuron-to-astrocyte signaling is central to the dynamic control of brain microcirculation. *Nat Neurosci*. 2003;6(1):43-50.
42. Belanger M, Allaman I, and Magistretti PJ. Brain energy metabolism: focus on astrocyte-neuron metabolic cooperation. *Cell Metab*. 2011;14(6):724-38.
43. Freeman MR. Specification and morphogenesis of astrocytes. *Science*. 2010;330(6005):774-8.
44. Tsai HH, Li H, Fuentealba LC, Molofsky AV, Taveira-Marques R, Zhuang H, Tenney A, Murnen AT, Fancy SP, Merkle F, et al. Regional astrocyte allocation regulates CNS synaptogenesis and repair. *Science*. 2012;337(6092):358-62.

Figure legends

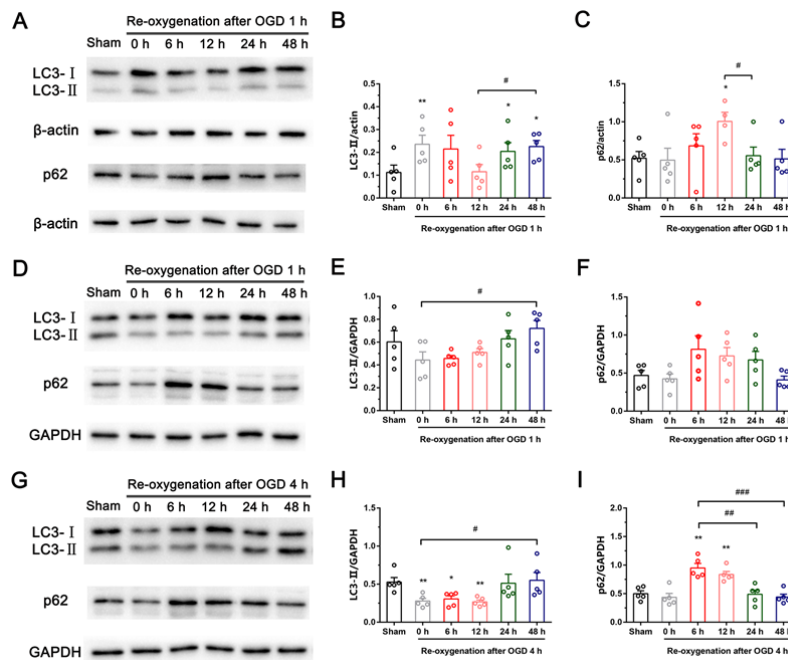


Fig 1. OGD and re-oxygenation changed levels of autophagy flux in neurons and astrocytes. A) Western blot showing the time course of autophagy flux in neurons from a sham group and after re-oxygenation for 0, 6, 12, 24, and 48 h following OGD for 1 h. B, C) Quantification showed that autophagy flux of neurons remained at low levels in sham group and was activated immediately upon exposure to OGD ($*P < 0.05$). Autophagy flux of neurons was inhibited after oxygenation for 12 h, decreasing to the baseline level. However, it increased again after oxygenation for 24 h and 48 h ($*P < 0.05$) ($n = 5$). D, G) Western blot showing the time course of autophagy flux in astrocytes from a sham group and after re-oxygenation for 0, 6, 12, 24, and 48 h following OGD for 1 h or 4 h. E, F) OGD 1 h and re-oxygenation did not change the autophagy flux level of astrocytes. H, I) Quantification showed that autophagy flux of astrocytes remained at high levels in the sham group. Autophagy flux of astrocytes was inhibited immediately upon exposure to OGD for 4 h and decreased to the lowest level after re-oxygenation for 12 h ($*P < 0.05$). It increased again after re-oxygenation for 24 h and 48 h, reaching baseline levels ($n = 5$). Results are presented as means \pm SEM.

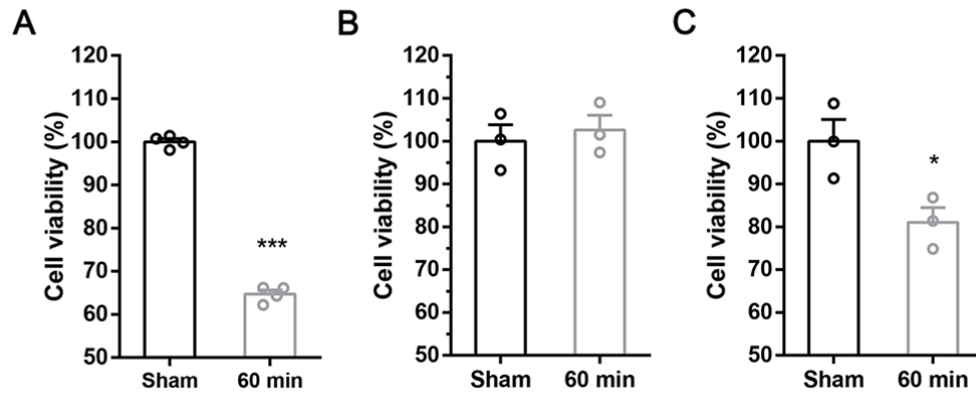


Fig 2. Astrocytes enhanced viability of neurons after OGD. A) Primary neurons were cultured alone and randomly divided into sham and OGD (60 min)/R (24 h) groups. A cell counting kit showed that neuronal viability was reduced significantly to 65% when subjected to OGD for 60 min when compared with OGD for 0 min ($***P < 0.001$) ($n = 4$). B) Primary astrocytes were cultured alone and divided into sham group and OGD (1 h)/R (24 h) groups. Results showed that astrocytes subjected to OGD for 60 min and re-oxygenation for 24 h showed no significant difference when compared with OGD for 0 min ($n = 3$). C) Neurons and astrocytes were co-cultured and divided into sham and OGD (1 h)/R (24 h) groups. Addition of astrocytes to neuronal cell cultures resulted in higher neuronal viability (80%) ($**P < 0.01$) when compared with OGD for 0 min, which is higher than that of neurons cultured alone ($n = 3$). Results are presented as mean \pm SEM.

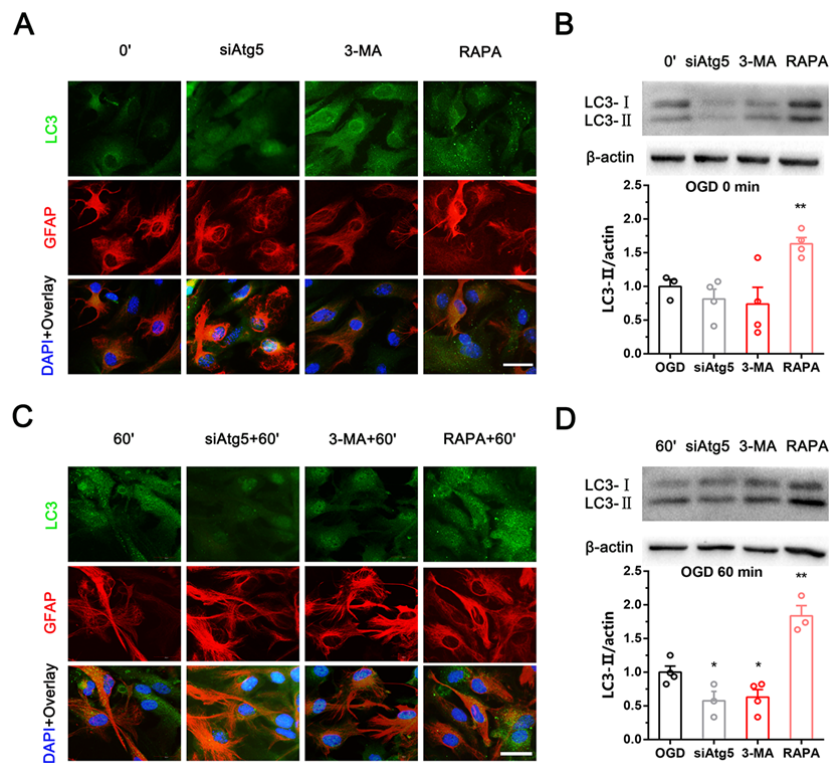


Fig 3. The effectiveness of regulating autophagy flux of astrocytes was observed dynamically. A, C) Strong, punctate LC3 staining was observed in the cytoplasm of astrocytes (GFAP) upon administration of RAPA in the OGD model (0 min, 60 min)/R (24 h), but not in 3-MA or siATG5. B, D) Representative immunoblotting of LC3 in control astrocytes and in administration of agents (3-MA or RAPA) or in siATG5 and its corresponding quantification showed that LC3- II to be increased in the astrocytes with administration of RAPA but decreased upon administration of 3-MA or in siATG5 in the OGD/R model (* $P < 0.05$; ** $P < 0.01$). Scale bar = 20 μm .

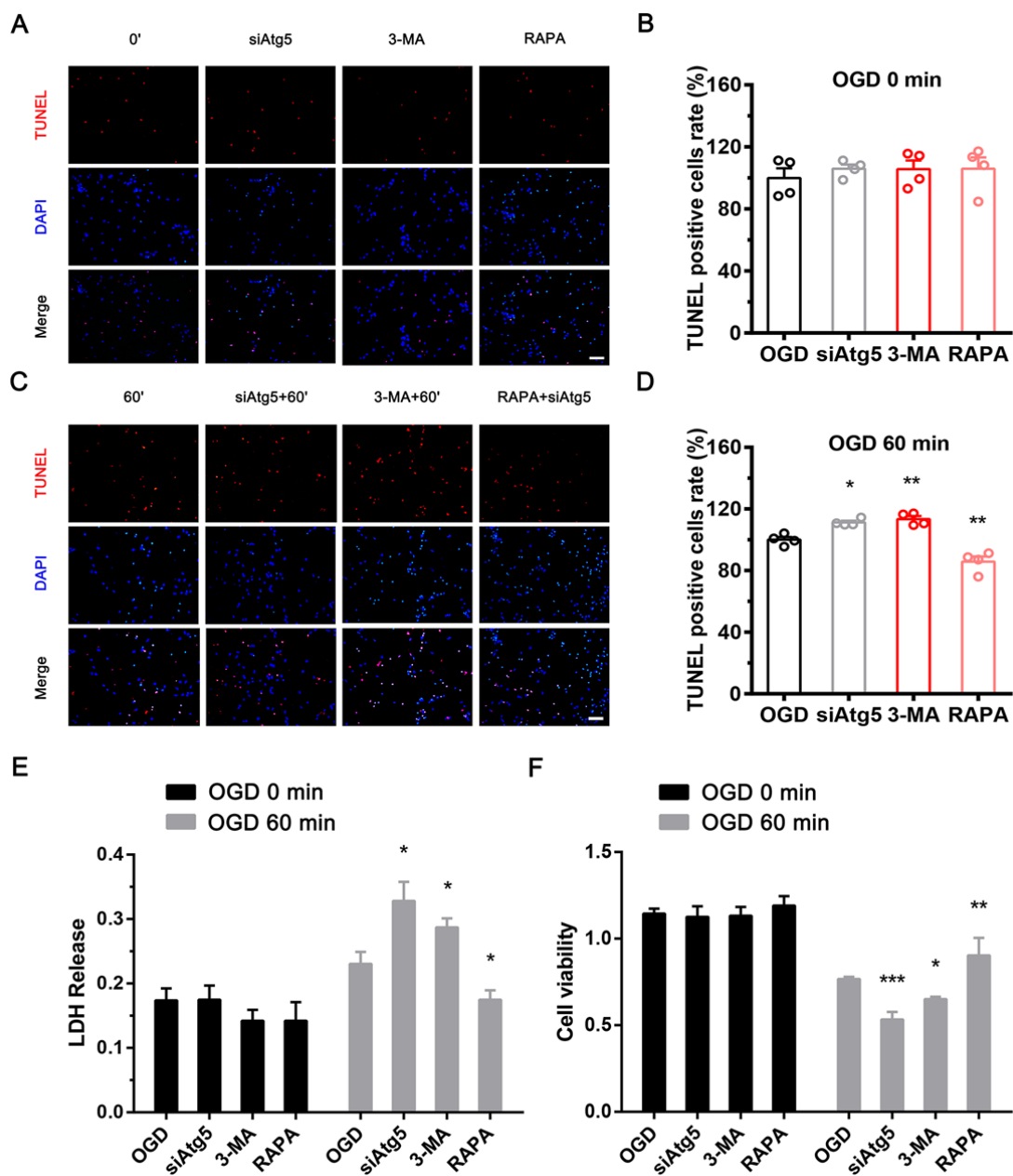


Fig 4. Induction of autophagy flux in astrocytes alleviated neuronal damage after OGD. From left to right, 4 groups of astrocytes, which were maintained under normal conditions and treated with siATG5, 3-MA, or RAPA, were co-cultured with neurons. After OGD, neuronal apoptosis, cytotoxicity of the co-culture system, and neuronal viability were measured by TUNEL staining, LDH assay and CCK8 assay, respectively. The percentage of positive cells was calculated as TUNEL-positive cells (number of positive cells / total number of cells × 100%). Four groups of astrocytes had no effect on neuronal apoptosis

rate (A), LDH release (C), and neuronal ability (E) in control groups. Induction of autophagy flux in astrocytes with RAPA reduced neuronal apoptosis rate (B) (** $P < 0.01$) and LDH release (D) and increased neuronal viability (F) ($*P < 0.05$). In contrast, inhibition of autophagy flux in astrocytes with 3-MA or siATG5 increased neuronal apoptosis rate (B) and LDH release (D) and decreased neuronal ability (F) ($*P < 0.05$) following OGD (60 min)/R (24 h) ($*P < 0.05$, $*P < 0.01$). These data are presented as mean \pm SEM (n = 4-5). Scale bar = 50 μ m.

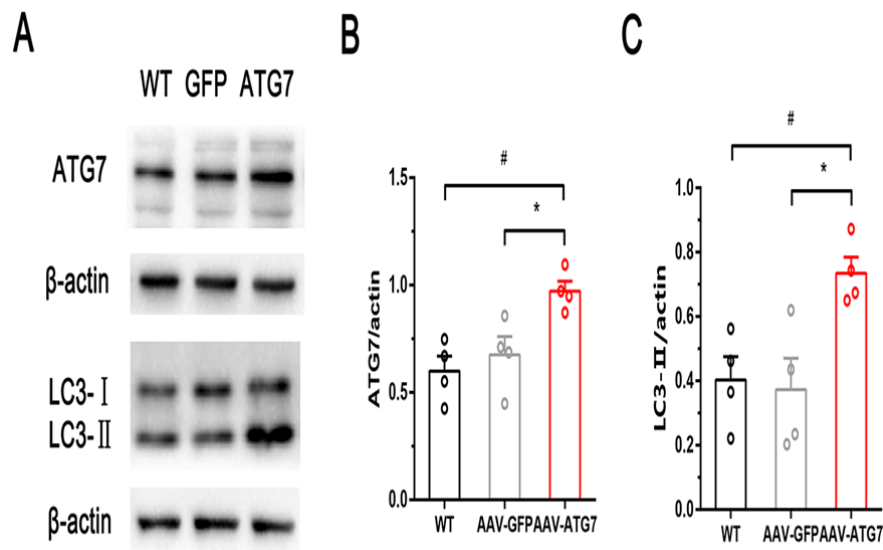


Fig 5. A–C) Immunoblotting of ATG7 and LC3- II in wild type, AAV-GFAP-GFP, and AAV-GFAP-ATG7 and corresponding quantification showed that autophagy was induced with AAV-GFAP-ATG7. These data are presented as mean \pm SEM (n = 4–5) (* P < 0.05; # P < 0.05).

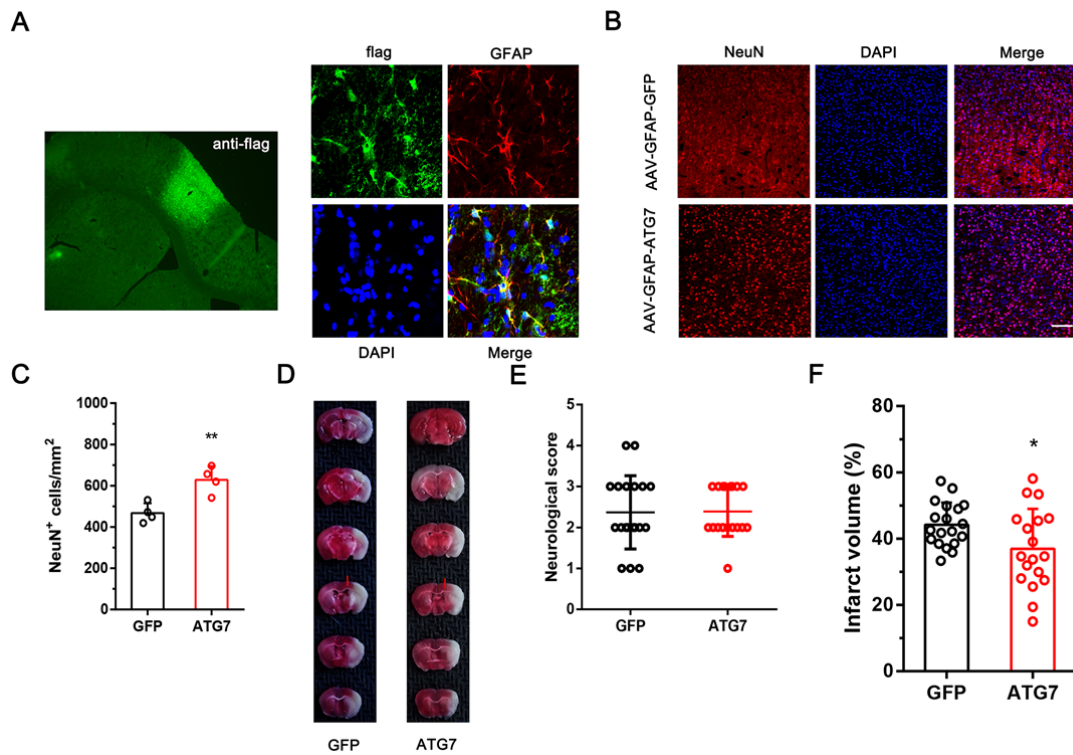


Fig 6. Induction of autophagy flux of astrocytes exerted neuroprotection after MCAO (1 h)/reperfusion (24 h). A) Immunostaining showing that the site of injection was correct and astrocytes were infected with AAV. B) Neuron-specific nuclear protein staining was used to measure survival of neurons in penumbra tissue. The results showed that upregulation of autophagy flux in astrocytes with AAV-GFAP-ATG7 increased survival of neurons in penumbra tissue following MCAO/reperfusion ($*P < 0.05$) ($n = 3$) (C). TTC staining of coronal brain sections at 24 h after reperfusion from mice treated with AAV-GFAP-GFP or AAV-GFAP-ATG7 ($n = 17-19$). The red rods indicate the location -1 mm relative to bregma, at which the AAV was injected. E) Neurological deficits were evaluated using the Longa scoring system ($n = 17-19$). F) The AAV-GFAP-ATG7 group had a significantly reduced infarct volume compared with the AAV-GFAP-GFP group ($*P < 0.05$ vs. GFP). Scale bar = 100 μ m.